# DETERMINATION OF THE DRAG COEFFICIENT OF LATTICE STRUCTURES UNDER WIND LOAD USING POROUS MEDIA APPROACH

by

***Milada L. PEZO*[*], *Nikola S. MIRKOV, and Vukman V. BAKIĆ***

Department of Thermal Engineering and Energy,
Vinča Institute of Nuclear Sciences, National Institute of the Republic of Serbia,
University of Belgrade, Belgrade, Serbia

Original scientific paper
https://doi.org/10.2298/TSCI210511233P

*The power transmitters, guyed masts and other lattice structures are exposed to wind action. The aerodynamic forces acting on tall tower constructions have crucial importance on the stability of the structure. The lattice structure drag coefficient determination is the subject of the international standards ESDU 81027 and 81028 and Eurocode 3 Part 3.1, but it can also be determined by numerical methods. For that purpose modelling using CFD proved to be both accurate and reliable. In this study the fluid-flow around the segment of a power transmitter was simulated by a 3-D model, where the geometry of the segment is approximated with a porous structure having the appropriate factor of porosity, in order to simplify the geometry. We have used three representative models of turbulence, standard k-ε model, RNG k-ε model, and Reynolds stress model. Drag coefficient values are extracted from the flow field and compared for all studied cases and with available experimental results from the wind tunnel. Simulations were performed for four wind velocities between 10 m/s and 30 m/s. The results are supplemented by the ones obtained by artificial neural network. The aim of this study is to show how the simple turbulence model coupled with approximated geometry can be used in the analysis of the aerodynamic forces acting on the lattice structure.*

Key words*: wind load, lattice structure, drag coefficient, porous material*

## Introduction

The lattice structures have a wide range of applications in engineering. Tall thin-walled structures made of steel elements can be used as power transmitters, meteorological guyed masts, in various steel constructions, *etc*. These structures are exposed to different climatic conditions and their stability is jeopardized by aerodynamic forces acting on the construction. Wind load is one of the most important design loads that can lead to permanent deformation of lattice structures, even its failure. Aerodynamic forces can be determined by experiments performed in wind tunnels or by numerical simulation.

Experimental and numerical analysis of the structural stability of the quartet steel-tube-column transmissionwer were investigated in [1]. These towers are used for higher and stronger ultra-high voltage long span transmission. Finite element method was used for structural and buckling analysis of the tower. A static non-linear buckling analysis for transmission-wer subjected to a wind load is conducted in [2]. The results of these investigations show that

[*] Corresponding author, e-mail: milada@vinca.rs

the uncertainty of material properties has the strongest influence on the stability of the tower. The influence of the dimensions of the structure elements and the wind attack angle was also discussed. It is shown that the most unfavorable wind attack angle is 0°, and that the most sensitive is the position in the middle of the tower body. Another investigation of the dynamic analysis of transmissionwer subjected to wind and rain loads given in [3], proposed a method for calculating the rain load based on the single raindrop impinging experiment. Lattice structures like guyed masts were also investigated in the past. Structural, modal and buckling analyses of the guyed mast have been thoroughly analyzed in [4].

There is a large amount of research concerning the determination of the drag coefficient for various models and shapes. Cheng [5] determined by two formulas for explicitly evaluating the drag coefficient and settling velocity of spherical particles in the entire subcritical region. Guo *et al.* [6] proposes a new formula for drag coefficient of cylindrical particles based on three parameters, the Reynolds number, and particle orientation angle and particle aspect ratio. Holzer and Sommerfeld [7] provides a new simple correlation formula for the drag coefficient of non-spherical particles fitting a large number of experimental data from the literature and a comprehensive numerical study. Numerical investigations of drag coefficient of circular cylinder with two free ends in roller bearings are performed in [8]. The drag force of the bridge section obtained by the global force and pressure distribution methods was the object of study in [9]. Determination of drag coefficient of lattice structure by using mathematical modelling of a flow around one segment of the guyed mast, conducted for a wide range of Reynolds numbers and for different angles of attack, is shown in [10]. Balczo *et al*. [11] show numerical simulations of flow around the telecommunication mast using CFD with RANS turbulence model.

There are a lot of experimental investigations done in wind tunnels of the drag coefficient values pertinent to current study. Lu *et al*. [12] performed the wind tunnel tests for mean drag and lift coefficients on multiple circular cylinders arranged in-line and examined the variation of drag coefficient *vs.* Reynolds number. Bakić [13] determined the drag coefficient of a sphere by the experimental investigation in the turbulent flow regime. Georgakis *et al*. [14] did a series of full-scale section model wind-tunnel tests of several lattice mast configurations and compared to Eurocode 3 standard. The dynamic response study of a 300 m tall, guyed telecommunication mast under various wind loads is conducted [15]. A formula is given in the same article, for calculating the drag coefficient based on the Canadian design standard [16].

For many technical research and engineering applications, determination of aerodynamic forces and drag coefficient is essential. Empirical expressions for the drag coefficient can be found in the literature and in the international standards such as ESDU 81027 and 81028 and Eurocode 3 Part 3.1 that processes the aerodynamic drag coefficient of lattice structures. The constructions with lattice structures can have complex geometry, difficult to use in numerical simulations. Simplification of the geometry can contribute to the usage of the less complex mesh for numerical modelling and facilitate computer simulation. Treating lattice structure as porous structure can shorten computer time and still can give accurate information about the drag force acting on the structure. Therefore, the porous structure method is implemented in the present study, employing the factor of porosity, which represents the ratio between the actual area and the modeled area. The porous structure representing the transmissionwer segment is embedded in simulated domain and three different turbulence models were used to reconstruct the flow field around it. Based on the flow field and reference parameters the drag coefficient is calculated subsequently. In addition, the simulations are compared with experiments performed in the wind tunnel for the wind velocities performed in the range between 11 m/s and 29 m/s [17]. The experiments were conducted in the wind tunnel in Rhode-Saint-Genese, Belgium.

The test section is 3 m wide and 2 m high. The velocity field in the wake of the lattice structure was measured by particle image velocimetry. The pressure sensors were placed in the wind tunnel and they supply the information about dynamic pressure and wind velocity. The motivation of this study is on method applied to determine the drag coefficient for lattice structure treated as porous structure. Prediction of the drag coefficient of the lattice structures can also be achieved by different numerical approaches, such as artificial neural network (ANN) modelling which will be shown here as a supplement to the CFD results.

## Description of the model

The transmissionwer is a tall lattice structure placed on the open and subjected to various climatic conditions. Wind load is one of the most important factors, which influence the stability of the transmissionwer. Determination of the aerodynamic force is crucial for engineering and scientific research. Mathematical modelling and numerical simulations can be used to analyze the fluid-flow around the lattice structure subjected to wind loading. The CFD approach proved to be an effective and reliable way to determine the aerodynamic force on the transmissionwer and can be used in its design to ensure its stability in exploitation. The geometry of this structure is very complex and it can lead to complex and demanding numerical simulations. The porous media approach used to treat geometry of the lattice structure as porous media can be used for the simplification the geometry and yet to save the information regarding aerodynamic forces and drag coefficient. Justification for treating the lattice structure as porous structure can be found in Maesschalck *et al.* [18]. The simulation of the flow around porous-like structures with the porous media approach instead of the detailed geometry can contribute to the much lower number of cells and simplify the numerical model. This approach is commonly used in wind engineering to evaluate the effect of vegetation on the wind flows [19, 20].

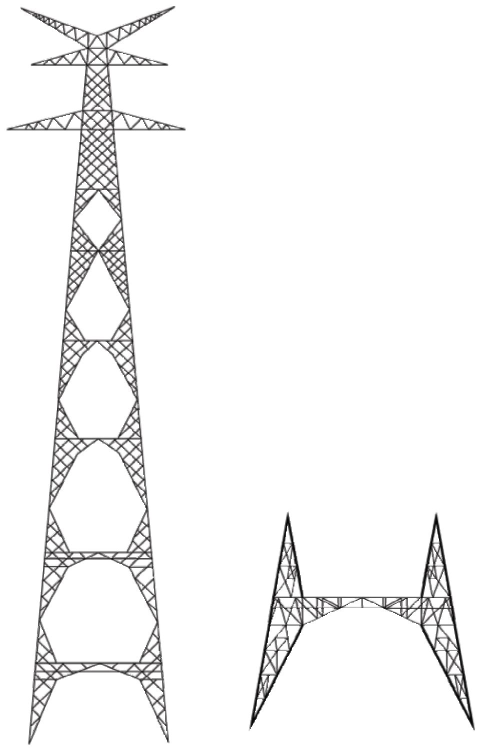

**Figure 1. The scheme of the structure of transmissionwer**

The transmissionwer is 192 m tall, is graphically represented in fig. 1. It consists of L-shaped lattice elements with different dimensions. The cross-sections of the main elements are square shaped. The simulated segment of the tower is 0.31 m tall and has a square cross-section 0.36 m long, made of steel, fig. 2(a). The geometry of the segment of the tower is very complex and porous media approach was used for the simplification of the geometry, fig. 2(b).

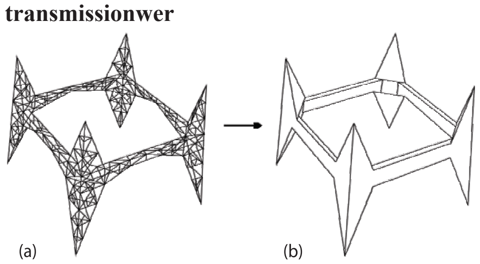


**Figure 2. The geometry of the lattice segment; (a) real segment and (b) approximated segment**

The fluid-flow around this 3-D porous segment is simulated, and the aim was to obtain the pressure field around it, which would approximate the pressure field near the original tower segment. Modelling of the fluid-flow around the lattice structure segment of the transmissionwer was conducted for wind velocities in the range from 10-30 m/s, which is slightly wider range than in reported measurements. Boundary conditions for this simulation are summarized in tab. 1.

**Table 1. Description of the boundary conditions**

| Boundary condition | Description of the boundary conditions |
|---|---|
| Inlet | Constant value for velocity, 10-30 m/s |
| Outlet | Pressure outlet, atmospheric pressure |
| Segment of the tower | Lattice structure – porous media |
| Other side of the volume | Line of symmetry |

## Mathematical model for CFD simulations

The equations of the viscous, incompressible fluid are assumed to govern the flow. The flow is considered turbulent, the Reynolds-Averaged Navier-Stokes form of the equations is invoked, and three distinct turbulence models were used for turbulence closure. Two models based on the eddy-viscosity concept are used, the standard *k-ε* model, and RNG *k-ε* model, and the third was the Reynolds stress model (RSM) turbulence model. We briefly summarize their formulation below, while for other details, one can see Wilcox [21] or theory guide [22], which are the references this short summary is based upon.

### *Standard k-ε model*

The standard *k-ε* model is a semi-empirical model and it is used to simulate the mean flow characteristics of turbulent flow conditions. This model solves two equations: transport equations for the turbulence kinetic energy, *k*, and transport equation for the rate of dissipation of turbulence energy, *ε*:

$$\frac{\partial}{\partial x_j}\left(\rho U_j k\right)-\frac{\partial}{\partial x_j}\left[\left(\mu+\frac{\mu_t}{\sigma_k}\right)\frac{\partial U_i}{\partial x_j}\right]=G_k-\rho\varepsilon \tag{1}$$

$$\frac{\partial}{\partial x_j}\left(\rho U_j \varepsilon\right)-\frac{\partial}{\partial x_j}\left[\left(\mu+\frac{\mu_t}{\sigma_\varepsilon}\right)\frac{\partial U_i}{\partial x_j}\right]=C_{1\varepsilon}\frac{\varepsilon}{k}G_k-C_{2\varepsilon}\rho\frac{\varepsilon^2}{k} \tag{2}$$

$$G_k=\mu_{\text{eff}}S^2,\ S\equiv\sqrt{2S_{ij}S_{ij}} \tag{3}$$

$$\mu_t=C_\mu\frac{k^2}{\varepsilon} \tag{4}$$

where $G_k$ is the generation of turbulence kinetic energy due to the mean velocity gradients, $C_{1\varepsilon}$, $C_{2\varepsilon}$, and $C_\mu$ are model constants, $\sigma_k$ and $\sigma_\varepsilon$ – the turbulent Prandtl numbers for $k$ and $\varepsilon$, respectively, and $\mu_\text{t}$ – the turbulent viscosity. The value of the constants are: $C_{1\varepsilon}$= 1.44, $C_{2\varepsilon}$= 1.92, $C_\mu$= 0.09, $\sigma_k$= 1.0, and $\sigma_\varepsilon$= 1.3 [22].

### *The RNG k-ε model*

The RNG model is analytically derived two-equation turbulence model, which differs from the standard *k-ε* model regarding the destruction of the dissipation term in the transport equation for turbulence kinetic energy dissipation rate, $\varepsilon$. In the RNG model the modification is accounted for using the modified constant:

$$C_{2\varepsilon}^{*} = C_{2\varepsilon} + \frac{C_\mu \eta^3 \left(1 - \dfrac{\eta}{\eta_0}\right)}{1 + \beta\eta^3} \tag{5}$$

where $\eta = Sk/\varepsilon$, $\eta_0 = 4.38$, and $\beta = 0.012$. The modified set of model constants are: $C_{1\varepsilon} = 1.42$, $C_{2\varepsilon} = 1.68$, $C_\mu = 0.0845$, $\sigma_k = 1.0$, and $\sigma_\varepsilon = 1.3$ [22].

### Reynolds stress model

The most complex classical turbulence model is the RSM. In the RSM eddy viscosity approach is abandoned and components of the Reynolds stress tensor are determined from transport equations for the Reynolds stresses and the equation for the dissipation rate. The exact transport equations for the transport of the Reynolds stresses are not reproduced here for brevity, and the readers are pointed to literature, *e.g.* [21, 22].

### Numerical method

The flow around the lattice structure is simulated using CFD software tool ANSYS FLUENT, based on the finite volume method. Flow field is considered statistically steady, placed in neutral atmospheric conditions, therefore, buoyancy effects are neglected. The pressure-velocity coupling is solved by semi implicit method for pressure-linked equations (SIMPLE) algorithm [23]. Discretization scheme for pressure is set to second-order. Discretization schemes for velocity components and turbulence scalars were set to second-order upwind. Cell-centered gradients were approximated using the least-squares method, with additional use of the default slope-limiter (Barth-Jespersen). The algebraic multigrid method with Gauss-Seidel smoother is used to solve the set of algebraic equations resulting from discretization of governing equations. The residual tolerance for the outer iterations was set to $10^{-5}$. The numerical Mesh is made of 156268 tetrahedral control volumes. Optimization of the grid and the grid refinement tests were performed to assure grid independence of the final solution. All three turbulence models, used for this study, are available in the standard package of ANSYS FLUENT.

The drag coefficient was determined by the FORTRAN code specially developed for this purpose.

### Artificial neural network model

In addition computational fluid dynamics model, an ANN in the form of a multi-layer perceptron model, with three layers (input, hidden, and output) was used in order to predict the drag coefficient of the lattice structures. Before the calculation, both input and output data were normalized to improve the behavior of the ANN, [24]. Broyden-Fletcher-Goldfarb-Shanno algorithm was used for solving the unconstrained non-linear optimization during the ANN modelling. A series of different topologies were used, in which the number of hidden neurons varied from 5-20, and the training process of the network was run 100000 times with random initial values of weights and biases. The coefficients of determination were used as parameters to check the performance of the obtained ANN model.

### Numerical results and the comparison with available experimental results

Lattice structures have complex geometry and this can be problematic for numerical simulations. The grid around the complex geometry must be refined and computer time and costs of the simulation will be high. To alleviate the problem, the geometry of the transmission-wer may be simplified by the porous media approach. Treating lattice structures as porous media can be justified, because it is similar to some applications in wind engineering concerning leafs and trees [19, 20]. The porosity factor can be determined:

$$\psi = \frac{A_{\text{real}}}{A_{\text{por}}} \tag{6}$$

where $A_{\text{real}}$ is the area of the real construction and $A_{\text{por}}$ – the approximated, increased area, fig. 2(b).

The numerical simulations were performed for the same geometry and the same conditions as the experiments in the wind tunnel [17]. Three different turbulence models were used for the mathematical modelling and the wind velocity is between the 10 m/s and 30 m/s.

The drag force acting on the lattice structure can be calculated:

$$F_D = \frac{1}{2} C_D \rho v^2 A \tag{7}$$

where $C_D$ is the drag coefficient, $\rho$ [kgm$^{-3}$] – the density of air, $v$ [ms$^{-1}$] – the inlet wind velocity, and $A$ [m$^2$] – the reference area. The reference area is the frontal area projected in flow direction.

The pressure fields on the surface of the porous structure, modeled with $k$-$\varepsilon$, RNG, and RSM turbulence models, and for wind velocity of 24.1 m/s are given in fig. 3 as a sample of produced results. This specific wind velocity value is interesting for illustration since one wind tunnel test was performed for the same wind velocity. The flow fields around the lattice segment for the central plane are given in fig. 4. Summary of the results of numerical simulations for wind velocities between 10 m/s and 30 m/s as well as the experimental results for same lattice structure are given in fig. 5. All simulation approaches were able to qualitatively represent the $C_D$ *vs.* Reynolds number dependence, although with varying success. The characteristic length scale for computation of the Reynolds number is the length of the structure. It is assumed that the aerodynamic roughness of the surface can be neglected.

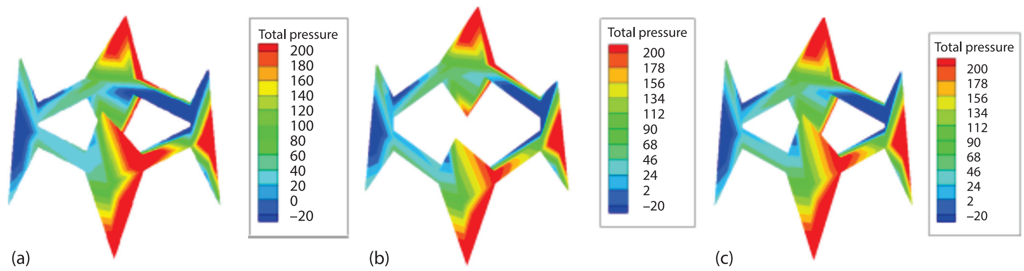


**Figure 3. Pressure field in the vicinity of the porous-like structure; (a) *k*-*ε*, (b) RNG, and (c) RSM turbulence model for wind velocity 24.1 m/s**

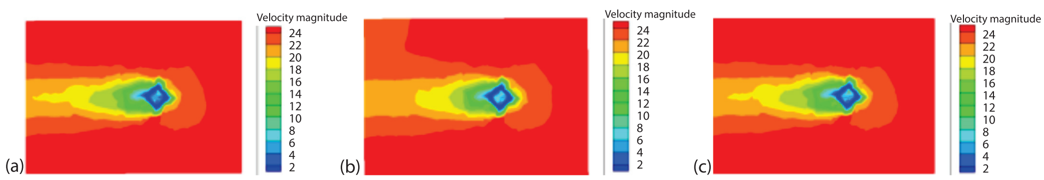


**Figure 4. Flow field for the central plane; (a) *k*-*ε*, (b) RNG, and (c) RSM turbulence model for wind velocity 24.1 m/s**

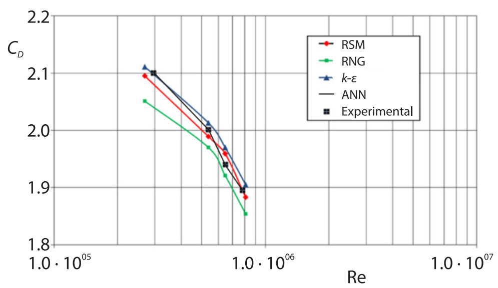


**Figure 5. Comparison of drag coefficient for four wind velocities based on different turbulence models and ANN model with experimental results**

The results of the computational simulations show good agreement with the experimental results. Firstly, it is clear that the Reynolds number has a strong influence on the values of the drag coefficient – the values of drag coefficient decrease with the increase of the Reynolds number. The values of the drag coefficient obtained from the numerical simulations show the overshoot for the standard *k-ε* model in the specified range, almost consistently, *i.e.* except for the lowest Reynolds number examined, where the experimental value lies on the fitted curve. For RNG *k-ε* model the line fitted to $C_D$ values from simulations shows consistent undershoot, and that model had the poorest performance on this problem. The Reynolds stress model is the only which showed change in pattern relative to experimental values, being slightly in undershoot for Reynolds number values up to Re = 600000, but this changes in the upper part of the range, only to be fitted ideally with measured value with the $C_D$ value at the highest end – the opposite behavior of the standard *k-ε* model. From this we can draw conclusions about the relative usefulness of the examined turbulence models.

The analysis of the agreement between the experimental results from the wind tunnel measurements [17] and the proposed computational and ANN models is given in tabs. 2 and 3. The quality of the fitting between the experimental results and the proposed models has been tested with a coefficient of determination, $R^2$, the reduced chi-square error, $\chi^2$, mean bias error (MBE), and root mean square error (RMSE). These commonly used statistical error norms could be calculated:

$$\chi^2 = \frac{\sum_{i=1}^{N}(x_{\mathrm{exp},i} - x_{\mathrm{pre},i})^2}{N-n} \tag{8}$$

$$RMSE = \left[\frac{1}{N}\sum_{i=1}^{N}(x_{\mathrm{exp},i} - x_{\mathrm{pre},i})^2\right]^{1/2} \tag{9}$$

$$MBE = \frac{1}{N}\sum_{i=1}^{N}(x_{\mathrm{exp},i} - x_{\mathrm{pre},i}) \tag{10}$$

where $x_{\mathrm{exp},i}$ is the experimental values, $x_{\mathrm{pre},i}$ – the values obtained from the proposed model, and $N$ – the number of tests and $n$ – the number of constants in the model. The criterion for the best agreement is: higher $R^2$ value, and lower $\chi^2$, MBE, and RMSE values.

**Table 2. Drag coefficient values for different Reynolds numbers, comparison of the numerical simulation results with the available experimental results**

| Reznolds number | Experiment | Reynolds stress model | RNG *k-ε* model | Standard *k-ε* model | ANN |
|---|---|---|---|---|---|
| $2.7 \cdot 10^5$ | 2.1 | 2.095 | 2.051 | 2.111 | 2.1 |
| $5.4 \cdot 10^5$ | 2.001 | 1.989 | 1.97 | 2.013 | 2.001 |
| $6.5 \cdot 10^5$ | 1.94 | 1.959 | 1.921 | 1.97 | 1.94 |
| $8.1 \cdot 10^5$ | 1.895 | 1.895 | 1.854 | 1.905 | 1.895 |

**Table 3. Statistical analysis of the results of the numerical simulation compared with available experimental results**

| Parameter | Reynolds stress model | RNG $k$-$\varepsilon$ model | Standard $k$-$\varepsilon$ model | ANN |
|---|---|---|---|---|
| $R^2$ | 0.990 | 0.982 | 0.989 | 1.000 |
| $\chi^2$ | $2.65 \cdot 10^{-4}$ | $2.70 \cdot 10^{-3}$ | $6.33 \cdot 10^{-4}$ | 0.000 |
| *MBE* | $-5.00 \cdot 10^{-4}$ | $3.50 \cdot 10^{-2}$ | $-1.58 \cdot 10^{-2}$ | 0.000 |
| *RMSE* | $2.65 \cdot 10^{-4}$ | $2.70 \cdot 10^{-3}$ | $6.33 \cdot 10^{-4}$ | 0.000 |

According to tabs. 2 and 3, the Reynolds stress turbulence model proved to be the most reliable computational turbulence model to predict drag coefficient values of the lattice structure. This is expected because the RSM takes into account most of the parameters that affect the flow regime and the pressure field. The least reliable model, according to present results given in the tab. 2 is the RNG model. The approximation of the lattice structure as a porous structure has small influence on the drag coefficient values. The porous structure approximation has greater influence on the flow field behind the object. It can be concluded from fig. 4 that the proposed model is not suitable for determination of the re-circulation zones around the structures, because the model did not catch the eddies around the porous-like object. Using real geometry instead of the porous-like geometry would improve the mathematical model and help better understanding of physical phenomena in this case. But it would also bring more complex numerical simulations, increase the number of cells used in the numerical mesh, increase time and costs of the computer simulations.

The ANN models predicted experimental values of the drag coefficient of the lattice structures reasonably well for a broad range of the Reynolds number values. The ANN model had an insignificant lack of fit tests, which means the model satisfactorily predicted output variables. A high $R^2$ value is indicative that the variation was accounted for and that the data fitted the proposed model satisfactorily [24].

## Conclusion

In this paper, we have showed the investigation of the wind flow through transmissionwers representing tall lattice structures exposed to varying wind conditions. Wind load is one of the most important factors affecting the stability of the construction, therefore, the determination of the aerodynamic drag force can be extremely interesting for the engineering practice. In this paper, we presented 3-D numerical simulations of the air-flow around the lattice structure. Three turbulence models based on Reynolds averaged Navier-Stokes approach (standard $k$-$\varepsilon$ model, RNG model and RSM) were used for the simulations. These three models coupled with the porous media model in which the lattice structure is simplified and approximated with the porous structure were used for numerical determination of the drag coefficient. The CFD simulation results correspond well to the wind tunnel measurements available in the literature. The treatment of the complex lattice structure by approximating it with the porous media proved to be justified in the numerical setting to a high degree of accuracy. This simplification can contribute to a less demanding computer simulation, in terms of computational resources required. Good matching of present computational results and available experimental results affirms present methodology for research and practical engineering purposes.

## Acknowledgment

This research was supported by the Ministry of Education, Science and Technological Development of the Republic of Serbia and Serbian-Slovenian bilateral project No. 337-00-21/2020-09/40.

## References

[1] Deng, H., *et al*., Experimental and Numerical Analysis on the Slope Change Joint of a Quartet Steel-tube-Column Transmissionwer, *Thin-Walled Structures*, *119* (2017), Oct., pp. 572-585
[2] Fu, X., Li, H. N., Uncertainty Analysis of the Strength Capacity and Failure Path for a Transmission-wer under a Wind Load, *Journal of Wind Engineering & Industrial Aerodynamics*, *173* (2018), Feb., pp. 147-155
[3] Fu, X., Li, H. N., Dynamic Analysis of Transmissionwer-Line System Subjected to Wind and Rain Loads, *Journal of Wind Engineering & Industrial Aerodynamics 157*, (2016), Oct., pp. 95-103
[4] Pezo, M., *et al*., Structural Analysis of Guyed Mast Exposed to Wind Action, *Thermal Science*, *20* (2016), Suppl. 5, pp. S1473-S1483
[5] Cheng, N., Comparison of Formulas for Drag Coefficient and Settling Velocity of Spherical Particles, *Powder Technology*, *189* (2009), 3, pp. 395-398
[6] Guo, X., *et al*., New Formula for Drag Coefficient of Cylindrical Particles, *Particuology*, *9* (2011), 2, pp. 114-120
[7] Holzer, A., Sommerfeld, M., New Simple Correlation Formula for the Drag Coefficient of Non-Spherical Particles, *Powder Technology*, *184* (2008), 3, pp. 361-365
[8] Gao, W., *et al.*, Numerical Investigations on Drag Coefficient of Circular Cylinder with Two Free ends in Roller Bearings, *Tribology International*, *123* (2018), Nov., pp. 43-49
[9] Han, Y., *et al.*, Numerical Analysis on the Difference of Drag Force Coefficients of Bridge Deck Sections between the Global Force and Pressure Distribution Methods, *Journal of Wind Engineering & Industrial Aerodynamics*, *159* (2016), Dec., pp. 65-79
[10] Pezo, M., Bakić, V., Numerical Determination of Drag Coefficient for Guyed Mast Exposed to Wind Action, *Engineering Structures*, *62-63* (2014), Mar., pp. 98-104
[11] Balczo, M., *et al.*, Prediction of Wind Load Acting on Telecommunication Masts, *Proceedings*, IABSE 2006 Annual Meetings and Symposium, Budapest, Hungary, 2006
[12] Liu, X., *et al.*, Wind Tunnel Tests for Mean Drag and Lift Coefficients on Multiple Circular Cylinders Arranged in-Line, *Journal of Wind Engineering and Industrial Aerodynamics*, *96* (2008), 6, pp. 831-839
[13] Bakić, V., Experimental Investigation of Turbulent Flows Around a Sphere, Ph. D. thesis, Technical University of Hamburg, Harburg, Germany, 2002
[14] Georgakis, C. T., *et al.*, Drag Coefficients of Lattice Masts from Full-Scale Wind-Tunnel Tests, *Proceedings*, EACWE 5, Florence, Italy, 2009
[15] Zhu, N., Wind Tunnel Test for Guyed Mast Dynamic Characteristics under Wind Loads, A Thesis Submitted to the College of Graduate Studies and Research in Partial Fulfillment of the Requirements, M. Sc. thesis, Department of Civil and Geological Engineering University of Saskatchewan, Saskatoon, Canada, 2007
[16] ***, Canadian Standards Association standard S37 2001 for Antennas, Towers and Antenna-Supporting Structures, 2001
[17] Allegrini, J., *et al*., Porous and Geometry-Resolved CFD Modelling of a Lattice Transmissionwer Validated by Drag Force and Flow Field Measurements, *Engineering Structures*, *168* (2018), Aug., pp. 462-472
[18] Maesschalck, J., *et al*., Conception of Very High Towers for Crossing the River Scheldt, International Council on Large Electric Systems, CIGRE, Paper B2-213. Paris, France, 2018
[19] Guan, D., *et al*., A Wind-Tunnel Study of Windbreak Drag, *Agricultural and Forest Meteorology*, *118* (2003), 1-2, pp. 75-84
[20] Manickathan, L., *et al*., Parametric Study of the Influence of Environmental Factors and Three Properties on the Transpirative Cooling Effect of Trees, *Agricultural and Forest Meteorology*, *248* (2018), Jan., pp. 259-274
[21] Wilcox, D. C., *Turbulence Modelling for CFD*, DCW Industries, La Canada, Cal., USA, 2006
[22] Patankar, S. V., *Numerical Heat Transfer and Fluid-flow*, Hemisphere Publishing Corporation, Washington, USA, 1980
[23] Kollo, T., Von Rosen, D., *Advanced Multivariate Statistics with Matrices*, Springer, Dordrecht, Germany, 2005
[24] Turanyi, T., Tomlin, A. S.. *Analysis of Kinetics Reaction Mechanisms*, Springer, Berlin Heidelberg, Germany, 2014

Paper submitted: May 11, 2021
Paper revised: June 5, 2021
Paper accepted: June 11, 2021